HAIL IMPACT RESISTANCE OF BUILDING MATERIALS

TESTING, EVALUATION, AND CLASSIFICATION

By Peter Flüeler

INTRODUCTION

In Switzerland each year, hailstorms cause substantial damage to building envelopes, and, over time, total losses show an upward trend. The use of a plastic ball to simulate hail impact started in Switzerland in 1970 when roofing membranes were competing against traditional roofing materials such as roof tiles. Standards such as SN 564 280[1] and the recommendations of building authorities and insurance companies referred to such procedures. In determining hail impact resistance (HIR), a 40-mm plastic ball is shot at a specified speed at the test specimen. Temperature-sensitive materials are cooled at the surface to 5°C (41°F) and positioned on a rigid and/or flexible support. Façade elements are fastened at an angle of 45° or 90° with regular fasteners and jointed to each other. The resultant damage is assessed for leakage and/or visual deficiencies.

Constant projectile properties, reproducibility, instant damage assessment, and time and costs savings are the advantages of the current test procedures. There are, however, various disadvantages in this procedure in regard to natural weather influences. In general, the density of plastic balls is higher than that of natural hailstones, and the fracture behavior is brittle for ice, elasto-plastic for plastic balls. This means that a plastic ball exerts higher energy than that occurring with a natural hailstone.

Figures 1 (above) and 2 (right) – Shapes and dimensions of collected hailstones that fell from a supercell near Lugano on June 21, 2007 (left; photo by F. Terrasi), and in the city area of Zurich on June 24, 2002 (right; photo by U. Spreiter). The diameter of the 2-franc Swiss coin is 27 mm (1.06 in).

HIGH MASS – LOW SPEED VS. LOW MASS – HIGH SPEED

The approach to this problem with reference to natural environmental conditions demands knowledge of the impact speed of a hailstone. It can be calculated from analytical evaluation or – as in recent times – from the use of measuring devices during a hailstorm. If a high-speed camera is available, the impact speed can be indirectly established by videotaping the impact.

EVALUATION OF IMPACT VELOCITY

At impact on the ground, hail appears to be of white color. This fact leads to the conclusion that the amount of trapped air in the ice is apparently rather high. With increasing size, however, sliced hailstones often show a shell-like structure. Within this structure, clear ice alternates with porous ice, resulting from many ups and downs in the turbulent air circulation within a storm supercell. Size of hailstone and aerodynamic drag coefficient (c_w) as determined by the hailstone shape have the strongest influence on impact velocity. See *Figures 1* and *2*.

$$v_{tH}=\sqrt[2]{\frac{4\cdot d_H\cdot g\cdot \rho_{ice}}{3\cdot c_w\cdot \rho_{air}}} \qquad \text{Eq 1}$$

$$E_{kin}= m\cdot v^2/2 \qquad \text{Eq 2}$$

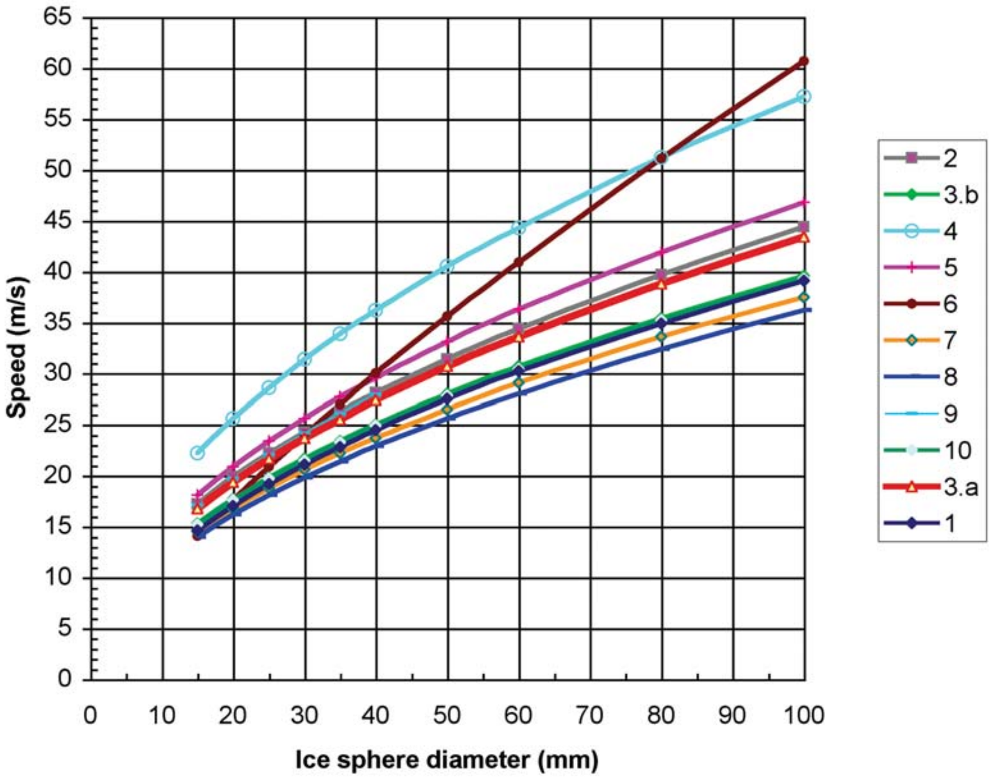

Figure 3 – Calculated terminal velocity for round hailstones from different authors. 1: Bohm; 2: ASTM 1038-05; 3a: EMPA with c_w 0.5; 3b: EMPA c_w 0.6; 4: Motz ρ_{air} 0.9 kg/m^3; 5: Motz ρ_{air} 1.23 kg/m^3; 6: Heymsfield; 7: Pflaum; 8 and 9: Matson; 10: Lozowski, Guastala, and Flüeler.

These shapes vary between round, egg-shaped, disk-like, smooth, warty, bulgy, and even extremely jagged-surfaced. Recently, bulgy, pointed forms were also detected in smaller-sized hailstones. Therefore, the c_w can range from 0.45 for a smooth surface to 0.80 for a rough surface. In turn, the density (r_{ice}) may range from 0.60 to 0.91 kg/dm^3.

In the past, various scientists have reported on hail impact velocity and its destructiveness. As an example, in 1937, Bilham and Relf[2] studied the differences between small (<10 mm or 0.40 in) and large hailstones. Motz[3], Kawashita/Flüeler[4], and others evaluated the most cited equations for terminal velocity. *Figure 3* shows the range of the calculated terminal velocity, v_{tH}, for hailstone diameters ranging from 20 to 100 mm (0.79 to 3.94 in). As a rule, factors in the calculation include the sphere diameter, d_H; the density of the ice, ρ_{ice}; the density of the air, ρ_{air}; and the coefficient of aerodynamic drag in air, c_w. The formula shown in *Figure 3* above is most frequently used.

In this present study, the following constants are used (*Figure 3*, curve 3a):

- Ice density at ρ_{ice}: 875 kg/m^3,
- Air density at 20°C ρ_{air}: 1.226 kg/m^3, and
- Coefficient of aerodynamic drag (c_w): 0.5 kg/m^2.

TEST PRACTICES OF COMMON STANDARDS

Since the beginning of recorded history, Australia, South America, the United States, and central Europe have known the effects of hailstorms. To toughen materials against hail impact, test procedures were first established in South Africa in the 1950s and in the United States at NIST in the 1960s. In Switzerland, the plastics industry provided evidence in the early 1970s that polymer roofing membranes are equal or even superior to classic roofing

Figure 4 – Test apparatus and tilted steel frame with mounting for a wood-framed window glass.

materials such as clay tiles in their resistance to hail impact. Initial impact testing was conducted using ice spheres.

Nevertheless, for practical and economic reasons, a 40-mm polyamide (PA) sphere was chosen. Comparisons of in-service hailstone damage on polymer roofing membranes to that obtained with the PA spheres showed similar damage patterns. Due to this fact, SIA established a test protocol in 1977[5] requiring a velocity of 17 m/s when shooting at a chilled waterproofing membrane supported by a steel plate and soft thermal insulation board (EPS). This velocity equates to a kinetic energy of 5.6 J. In comparison, good classic clay tiles become damaged at a velocity of 9 m/s, which is equal to 1.6 J.

TEST PROGRAM

To simulate the conditions of natural hail and its impact on the building envelope, an extensive experimental investigation was performed. A comparative study was carried out on 50 types of materials originating from 11 fields of application using laboratory-made ice spheres and plastic balls.

TEST APPARATUS AND PARAMETERS

The test apparatus consisted of a pneumatic gun positioned vertically (*Figure 4*). This apparatus was originally designed for use with plastic balls only. In the course of expanding our technical investigations, the apparatus was modified to launch 15- to 50-mm ice spheres. By using a light beam, the projectile velocity is instantaneously measured at the end of the gun barrel at a distance of 30 cm. Target and distance are aimed exactly by two focusing lasers. The velocity is set by the pneumatic pressure corresponding to calibration values enabling a repeatability of <1 m/s. See *Figures 5* and *6*.

Figure 5 – To condition the clay tile probe before testing, it is moistened three times with a wet sponge.

Figure 6 – Impacting a 50-mm ice sphere on a framed 7-mm-thick wire glass window.

For the project, the following parameters were chosen:

1. **Set-up of test specimen:** Condition new, as installed in building, custom-designed.
2. **Size of test specimen:** 0.8 to 1.1 m^2 with jointing, possible overlaps, and original fasteners.
3. **Surface treatment:** Temperature-sensitive materials chilled with ice granules for three minutes.
4. **Test temperature:** Room temperature and humidity, approximately 23°C/50% r.h.
5. **Impact angle:** Roofing, 90°, and façade, 45°; both applications 45° + 90°.
6. **Type of impact:** Single-shot mode.
7. **Impact speed:** Appropriate speed for size of projectile.

PROJECTILES AND PROPERTIES

For projectiles, precision balls made from PA 66 (density of 1.16 kg/dm^3) and laboratory ice spheres (density 0.875 g/cm^3) were used. The ice spheres were made in silicon molds using demineralized water. The production of crack-free and essentially pore-free ice spheres required approximately 17 hours at -20°C in a freezer. Freezing of the water was induced by a freezer plate at the bottom of the mold, thus facilitating slow growth of the ice core from bottom to top. Due to time-dependent changes of ice, a shelf time of less than three weeks was observed for the newly made ice spheres. The important properties of both types of projectiles are listed in *Table 1*.

PROCEDURE

To investigate the damage mechanism and weak points, test specimens were first impacted using PA balls fired within the velocity range observed for real hailstones at impact. At a damage velocity considerably higher or lower than natural velocities, test specimens were impacted by sphere sizes 10 mm higher or lower. Then, the procedure was applied by using ice spheres.

DAMAGE ASSESSMENT AND EVALUATION

Assessment of damage in regard to insurance codes of practice was the most challenging task. The diversity of materials, supports, substrates, and fastenings, along with the wide-ranging damage characteristics at impact, demanded very close examination of each application. Therefore, the damage characteristics due to impact were grouped within the following general categories:

1. **Loss of a main function:** such as watertightness, breakdown of mechanical/electrical properties, loss of load-bearing property, etc.
2. **Deformation:** indentation, dent formation, deformation of defined depth.
3. **Cracking and fracture:** visible cracks, spontaneous fracture, delamination.
4. **Aesthetics:** change of appearance, loss of light transmission, view in back light from a distance of 5 m.
5. **Damage affecting aging:** inherent cracking, face separation, debonding, and damage of surface layers.

After impact, the damage category was assigned based on the lowest velocity (i.e., kinetic energy according to Equation 2) that

TABLE 1 – MASS OF ICE SPHERES AND PLASTIC BALLS FOR VARIOUS DIAMETERS

TYPE OF SPHERE	UNIT	DIAMETER (MM)				FAILURE BEHAVIOR
		20	30	40	50	
Mass of ice	(g)	3.8	12.3	30.2	58.3	brittle
Mass of Polyamide	(g)	4.8	16.1	38.8	74.9	tough

TABLE 2.1 – HIGH-STIFFNESS, TOUGH MATERIALS

Material/ Component	Element Stiffness	E·I (kN•mm^2/mm)	Angle (°)	E_{kin} (J)	HIR Class	Lowest Values for		
						Product	Ø (mm)	E_{kin} (J)
Tiles	high	2330 - 2635	90	13.7 - 27.3	4	clay tiles	50	13.75
Glass	high	370 - 3000	45	5.5 - 46.7	3 - 5	wire glass 7	40	5.5
Fiber cement	high	140 - 252	45/90	17.6 - 38.2	4 - 5	corrug. plate 5.5	40	17.6
Polymer plates	high	0.3 - 9.6	90	6.4 - 38.8	3 - 5	PMMA 4	30	6.4
Skylights	high	5.3 - 7.4	90	0.8 - 3.1	2 - 5	PMMA 2.5	30	0.8
GRP boards	high	6 - 88	45	1.4 - 20.5	2 - 3	GRP-UP struct.	30	1.4

TABLE 2.2 – LOW-STIFFNESS MATERIALS, NON LOAD-BEARING

Material/ Component	Element Stiffness	E·I (kN•mm^2/mm)	Angle (°)	E_{kin} (J)	HIR Class	Lowest Values for		
						Product	Ø (mm)	E_{kin} (J)
Shutters	very low	0.1 - 4.2	45/90	0.05 - 1.75	1 - 2	profile, foam 0.25	20	0.05
Roller blinds	very low	0.5 - 1.2	45/90	0.2 - 0.7	1 - 2	folded 0.45	20	0.2
GRP: corrug., trapez.	low	1.95	90	0.4 - 0.5	1	GRP-UP trp. 1.4	20	0.4
Metal sheets, façade	low	1.9 - 2.6	45	0.6 - 1.7	1 - 2	alu 0.7	30	0.6
Membrane: stiff*	medium	0.001 - 0.6	90	39 - 90	5	SBS 3.7 sand coat	50	> 80
Membrane: soft*	medium	0.001 - 0.6	90	12.9 - 53.3	4 - 5	SBS 3.7 sand coat	40	12.9

TABLE 2.3 – MEDIUM-STIFFNESS MATERIALS

Material/ Component	Element Stiffness	E·I (kN•mm^2/mm)	Angle (°)	E_{kin} (J)	HIR Class	Lowest Values for		
						Product	Ø (mm)	E_{kin} (J)
Larch wood	medium	1.7	45	0.6 - 1.8	1 - 2	coated	30	0.6
Spruce wood	medium	1.5	45	0.8 - 3.1	2	planed	30	0.8
EIFS**	medium	1.7 - 2.8	45	5.7 - 17.0	3 - 4	EPS 20, 4	30	5.7
Metal sheets, roof	medium	2.1 - 6.0	90	0.6 - 2.0	1 - 2	cupper, 0.6	30	0.6

**Membrane placed on stiff/soft substrates, respectively*

***External Insulation and Finishing Systems (EIFS)*

resulted in damage. For ductile materials such as metallic sheets, the formation of a dent was judged to be aesthetic damage. In general, aesthetic damage was not observable until the depth of the indent reached about 0.5 mm.

RESULTS

The diversity of the investigated materials and their uses generated a wide range of results. Nevertheless, these results could be classified into three material categories according to load-bearing behavior, i.e., stiffness (*Tables 2.1 - 2.3*). A condensed report is provided by the Swiss Association of Fire Insurance Companies VKF[6], also in French.

Figure 7 is a plot relating depth of indentation to projectile kinetic energy for the case of a 0.7-mm zinc-plated, corrugated

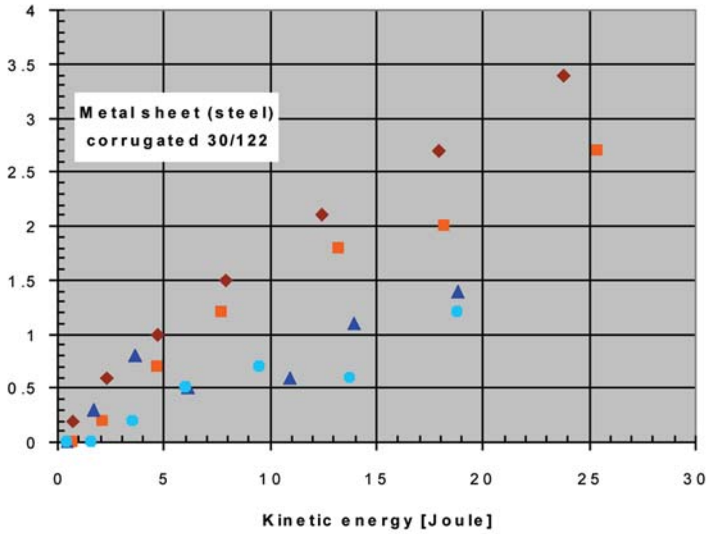

Figure 7 – Indentation versus kinetic energy (J) of a corrugated 0.7-mm steel sheet tested using 40-mm PA balls and 40-mm ice spheres.

Figure 8 – Indentations caused by 40-mm projectiles. Impact using PA balls (left) and ice spheres (right) at velocities of 26, 30, and 36 m/s.

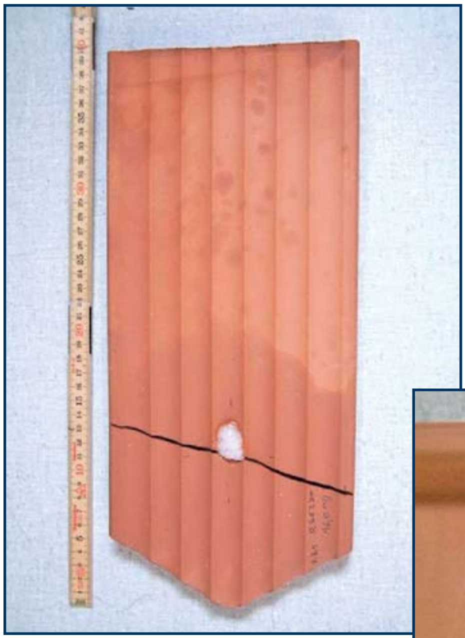

Figure 9 – Fractured clay tiles caused by 40-mm ice spheres: beaver's tile with center shot at 24.4 J (above); plane tile with corner shot at a kinetic energy of 25.8 J (right).

steel sheet impacted with 40-mm PA balls and 40-mm ice spheres. *Figure 8* shows a photo of the indentations at projectile velocities of 26, 30, and 36 m/s.

At a 90° impact angle, both projectile types caused circular indentations that increased in size with increasing velocity. At an angle of 45°, mainly ellipsoidal indents resulted. Upon impact, PA balls remained intact and showed no cracking. In contrast, ice spheres tended to split – even at a velocity as low as 10 m/s – depending on the nature, mass, and surface topology of the specimen. A clear observation from the testing was that for heavy mass specimens such as clay tiles, the ice fragmentation pattern was distinct and more diverse, changing with increasing velocity in comparison to the fragmentation of compliant specimens. A heavy-mass specimen is one for which the ratio of the test specimen mass to the projectile mass is greater than 50. Another observation was that low HIR values (i.e., <3 J) were, in general, found for specimens where the damage was categorized as aesthetic rather than functional. See *Figures 8* and *9*.

CORRELATION OF DATA FROM PA AND ICE SPHERES

Test data from two projectile materials – ice versus PA – allow a correlation of the tested materials. A ratio can be calculated between the values of velocity (and also kinetic energy) of ice spheres and PA ball spheres. *Figure 10* shows the relationship between the primary kinetic energy data for various specimens tested using 40-mm PA balls and 40-mm ice spheres.

This figure clearly confirms that many specimens experienced damage at very low kinetic energies. It is noted that hailstones having diameters less than 30 mm generally have kinetic energies of less than 3.5 J. Most importantly, from *Figure 10*, it is evident that the data points for many specimens fell well below or above the correlation line, indicating for these cases that testing needs to be conducted with ice spheres and not with PA balls. This is especially the case for roofing membranes tested on rigid substrates and for clay tiles.

CLASSIFICATION AND DESCRIPTION

A classification of building materials should be understood not only by material scientists and professionals in the building business, but also by users. So, it should be easy to understand and related to the observed weather phenomena. In a 1991 publication, Flüeler[7] made an attempt to define a classification system, including five levels of HIR. It is now stated to classify hail impact resistance into classes 1 to 5 (*Table 3*), which correspond to hailstone diameters of 10 to 50 mm where the building materials remain damage-free. It includes the corresponding terminal velocity of an impacting hailstone as calculated using Equation 1, curve 3a, of the

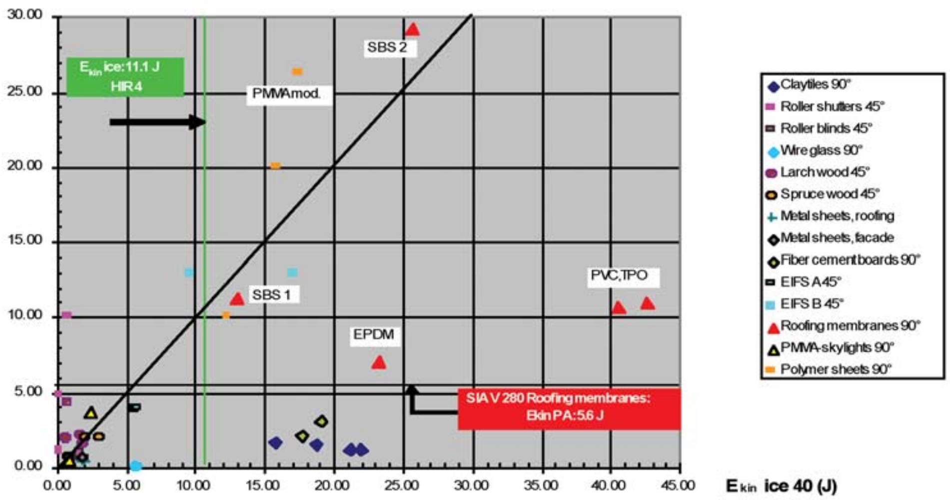

Figure 10 – Kinetic energy in J for ice spheres and PA balls causing damage. Actual requirement (red) for roofing membranes in Switzerland and new requirement for HIR Class 4 materials.

plot in *Figure 3*, and calculated maximum kinetic energy using Equation 2. An examination of *Table 3* shows that for each HIR class, the range of kinetic energy corresponding to that given HIR Class is rather large, ranging from 11.1 J to <27.0 J for HIR Class 4, for example. This realization dictates that for a more precise description, differences in kinetic energy sustained without damage must be taken into account in the proposed classification system.

The classification thus signifies not only the HIR class designation, but also the highest kinetic energy achieved without damage for the given sized ice sphere. *Table 4* provides HIR Class designations (without kinetic energy) for the specimens in this study.

CONCLUSIONS

This study confirmed field observations – particularly from insurance companies – that indicate that considerable hail damage payment (>80%) is made for the materials that fall within HIR classes 1 and 2. They experience damage at kinetic energies of 0.7 J or less.

Impact of stiff, high-mass construction materials by a PA ball provokes considerably higher kinetic energy than that of an ice sphere of the same size. The fragmentation energy is not available for the damage process. For very stiff and high-mass materials, an ice sphere must have a kinetic energy up to 15 to 20 times greater than that of a PA ball to inflict damage.

With the exception of mass difference, lightweight elastic materials behave almost similarly with the two types of projectiles because of low fracture/deformation energy absorption.

For materials with structured cross sections with thin faces (e.g., double face plate, <1 mm), a smaller projectile diameter might provoke damage, while a larger diameter causes no damage.

Due to the diversity of materials and systems used for building envelopes, HIR evaluations have to be performed using ice spheres impacting at natural terminal velocity. Moreover, the kinetic energy sustained during these evaluations has to be taken into account in an HIR classification system.

TABLE 3 – CLASSIFICATION OF HAIL IMPACT RESISTANCE (HIR) AND CALCULATED MAXIMUM KINETIC ENERGY

HIR CLASS	ICE SPHERE DIAMETER (MM)	MASS (G)	TERMINAL VELOCITY (M/S)	KINETIC ENERGY (J)
1	10	0.5	13.8	***0.04***
2	20	3.6	19.5	***0.7***
3	30	12.3	23.9	***3.5***
4	40	29.2	27.5	***11.1***
5	50	56.9	30.8	***27.0***

TABLE 4 – HIR GUIDE VALUES OF TESTED BUILDING MATERIALS AND PREDOMINANT DAMAGE CATEGORY

HIR CLASS	MATERIAL/COMPONENT	TYPE	THICKNESS (MM)	PREDOMINANT DAMAGE CATEGORY
1	roller shutters, roller blinds	aluminum, folded	< 0.5	deformation, aesthetics
	metal sheets	copper, tin	< 0.6	deformation, aesthetics
	GRP panels	light, shaped	> 2	fiber matrix defect
2	metal sheets, façade and roofing	Fe, Cu-Fe, Ti plated	> 0.5 - 0.7	deformation, aesthetics
	reinforced roller shutters	aluminum	0.9	deformation, aesthetics
	wood panels	planed, coated	25	indent, cracked paint
3	Skylights	PMMA	2.5	fracture, leakage, transparency
	GRP double-faced panels	structural	20	fiber matrix defect
	EIFS (EPS and rock wool)	reinforced glass web	> 3	cracking, debonding
	wire glass	wire net, 10 mm	7	fracture
4	roofing membranes	EPDM, SBS	4	leakage
	polymer sheets	PMMA modified	4	transparency, defect
	roof tiles	clay, structured surface	15	internal fissure (sound check)
	fiber cement boards/roofing	flat, undulated	6	indent, surface crack, fissure
5	roofing membranes	TPO, PVC-P	> 1.5	leakage
	polymer sheets, skylights	PC, plain + structured	4	deformation
	safety glasses	single, laminated	6	splitting, fracture
	window glasses	insulated, aluminum-framed	4/16/4	splitting, fracture

Note: HIR classes in this table are examples achieved in the study and should not be taken as requirements or guide values.

Very often, hail damage resulting in loss of function or other physical characteristics is not as disconcerting as aesthetic damage. As an example, car bodies dented by hail are still roadworthy.

The effect of hail impact on aging behavior must be sufficiently taken into consideration.

ACKNOWLEDGEMENTS

The research detailed herein was funded by the prevention fund of the Swiss Cantonal Building Insurance Association. The author wishes to acknowledge the various contributions from the building material industries and the support of the EMPA laboratories, mainly polymer and composites. Thanks to Thomas Egli, the main project leader, and to Maja Stucki and Fabio Guastala, coworkers at EMPA. Thanks also to Walter Rossiter for his English review and comments.

REFERENCES

1. SIA, *Polymer Waterproofing Membranes/Kunststoff-Dichtungsbahnen*, Swiss Association of Engineers and Architects, standard SN 584 280, editions 1977, 1988, 1996.
2. E.G. Bilham and E.F. Relf, “The Dynamics of Large Hailstones,” *Symon's Meteorological Magazine*, pp.149-162.
3. H.D. Motz, *Hagelrisiko - eine sicherheitswissenschaftliche Studie von Kausalität und Effekt*, PhD thesis, Univ. Gesamthochschule Wuppertal, D 468, Wuppertal, Germany, 1986.
4. L. Kawashita and P. Flüeler, simulated hail impact tests with ice and polyamide spheres, internal research report Empa no 860'091/2 (not public), August 20, 2002.
5. SIA
6. Swiss Association of Fire Insurance Companies VKF, Bern, *Elementarschutzregister Hagel, Synthesebericht*, Untersuchungen zur Hagelgefahr und zum Widerstand der Gebäudehülle, July 2007, 32 pages.
7. P. Flüeler and F. Rupp, “The Hail Impact Resistance of Plastic Components of the Building Shell,” *Proceedings, 3rd International Conference on Durability of Building Materials*, Bournemouth, England, 1988.

This paper was originally published in the Proceedings of the 11DBMC International Conference on Durability of Building Materials and Components, *Istanbul, Turkey, May 11-14, 2008.*

Peter Flüeler

Peter Flüeler is the founder of FPC Flüeler Polymer Consulting GmbH, Aathal, Switzerland. He received his masters in civil engineering from the Swiss Federal Institute of Technology (ETHZ) in Zurich and did postgraduate studies at MIT, Cambridge, MA, on polymers and composites. In the early 1970s, he was a structural engineer with Stocker Engineering, Bern. Later, he worked in the civil and mechanical engineering department of the Swiss Federal Laboratories for Materials Testing and Research (EMPA), and he has served as a lecturer at ETH Zurich. He was engaged as an expert in waterproofing and drainage of tunneling during construction of the Alptransit. Flüeler has authored and coauthored over 125 articles and holds two patents. He may be reached at p.flueler@hispeed.ch.